

kinetically difficult to dehydrate the oxonium ion to the ether at ambient temperature. However, the silyl ether intermediates (for example, a 2-propyl silyl ether from propene) may still be reached from the olefin side since this chemistry is more exothermic. Therefore, for the primary and secondary alcohols, the oligomerization chemistry characteristic of the olefins is not observed in our experiments.<sup>3,4</sup> In general, this type of diagram provides a useful framework for describing the link between alcohol reactants and complex hydrocarbon products via spectroscopically detectable reaction intermediates over H-ZSM-5.

#### Summary

The <sup>13</sup>C NMR spectrum of the intermediate formed from the adsorption and subsequent dehydration of 2-methyl-2-propanol

on H-ZSM-5 at 295 K shows that the intermediates can best be described as silyl ethers in which an alkyl group is covalently bound to the zeolite lattice. No peaks were observed in <sup>13</sup>C NMR spectra that could be attributed to carbenium ions, although all of the results are consistent with the formation of an equilibrium between a silyl ether and a carbenium ion. This silyl ether intermediate undergoes the same oligomerization chemistry found with simple olefins in H-ZSM-5, implying that it is also important in olefin reactions on H-ZSM-5.

**Acknowledgment.** We are grateful to the Mobil Oil Corp. for supplying us with the ZSM-5 zeolite.

**Registry No.** 2-Methyl-2-propanol, 75-65-0.

## Steric Effects and Threshold Rotational Mechanisms in 1-Substituted 2,2-Dimesitylethenols<sup>1</sup>

Silvio E. Biali,\* David A. Nugiel, and Zvi Rappoport\*

Contribution from the Department of Organic Chemistry, The Hebrew University of Jerusalem, Jerusalem 91904, Israel. Received January 27, 1988

**Abstract:** The static and dynamic stereochemistry of 1-alkyl- (and 1-H) 2,2-dimesitylethenols (Mes<sub>2</sub>C=C(OR<sub>2</sub>)R<sub>1</sub>) is studied and analyzed. The low-temperature <sup>1</sup>H NMR data for the enols are in agreement with a propeller conformation in solution. A <sup>1</sup>H dynamic NMR study shows that **1** (R<sub>1</sub> = R<sub>2</sub> = H) behaves differently from the other enols: enol **1** shows *two* different processes for the exchange of groups at each mesityl ring ( $\Delta G^{\ddagger}_c = 10.4$  and  $14.2$  kcal mol<sup>-1</sup>). The 1-alkyl-substituted enols **2-5** (R<sub>1</sub> = Me, Et, *i*-Pr, *t*-Bu; R<sub>2</sub> = H) display a single measurable barrier, which decreases with the increase of the bulk of the R<sub>1</sub> substituent. Substitution of the enolic hydrogen of **1** by an isopropyl group affords the enol ether **6** (R<sub>1</sub> = H; R<sub>2</sub> = *i*-Pr). From comparison of the enantiomerization barrier and the mesityl rotational barrier in either **4** or **6** it is concluded that the threshold rotational mechanism is the one-ring flip for **1** and **6** and the two-ring flip for **2-5**. These conclusions are strengthened by molecular mechanics calculations on **1** and **2** that satisfactorily reproduce their experimental rotational barriers. The rotational barriers for the two-ring process of **1-5** are linearly correlated with Taft's *E*<sub>s</sub> values, with  $\phi_2$  (the torsional angle of the ring *cis* to R<sub>1</sub>), and with  $\alpha_4$  (the C=C-R<sub>1</sub> bond angle). The two latter relationships with the structural parameters represent dynamics-structure correlations, and from that with  $\phi_2$  a crude estimate of this  $\phi_2$  torsional angle in the transition state of the two-ring flip process is obtained.

Triarylvinyl systems Ar'ArC=C(Y)Ar'' (Y = OH, H, Cl, OAc, OR) exist in a propeller conformation where the aryl groups (the propeller "blades" radiating from the double bond) are all twisted in the same sense.<sup>2-4</sup> When all the rings are identical and have local C<sub>2</sub> axis, these systems exist solely in two enantiomeric forms (assuming an effective conical symmetry of the Y substituent). These enantiomeric forms can be viewed as differing in helicity, i.e., in the sense of twist of the rings.<sup>5</sup>

The "vinyl propellers" display correlated rotation of the aryl rings, which can be conveniently analyzed in terms of "flip" mechanisms. In these mechanisms<sup>6</sup> (all involving helicity reversal) the ring which "flips" passes through a plane perpendicular to the ideal double bond plane, while the remaining rings rotate concurrently, disrotatorily, in the opposite direction and pass through the double bond plane. Depending on the number of flipping rings

the different flip mechanisms are designated zero-, one-, two-, or three-ring flip.<sup>7</sup> In contrast with molecular propellers of the type Ar<sub>3</sub>Z and Ar<sub>3</sub>CX (Z = C, B, or N; X = H, Me, or halogen) for which the rotational mechanism of lowest activation energy (threshold mechanism) is the two-ring flip,<sup>8</sup> the trimesitylvinyl propellers Mes<sub>2</sub>C=C(Y)Mes (Mes = 2,4,6-Me<sub>3</sub>C<sub>6</sub>H<sub>2</sub>) display a substituent-dependent threshold mechanism. When the double bond substituent Y is hydrogen, the threshold mechanism is the [ $\alpha,\beta$ ]-two-ring flip<sup>4</sup> (in which the  $\alpha$  ring and the  $\beta$  ring trans to the Y substituent "flip") whereas for bulkier substituents (Y = OH, Cl, OAc, OPr-*i*) the threshold mechanism is the three-ring flip.<sup>2</sup> The difference in the threshold mechanism was ascribed

(7) Examples of the idealized transition states for the flip mechanisms of a triarylvinyl propeller are depicted in Figure 3 of ref 2.

(8) (a) Mislow, K. *Acc. Chem. Res.* **1976**, *9*, 26. (b) Bye, E.; Schweizer, W. B.; Dunitz, J. D. *J. Am. Chem. Soc.* **1982**, *104*, 5893. (c) Wille, E. E.; Stephenson, D. S.; Capriel, P.; Binsch, G. *J. Am. Chem. Soc.* **1982**, *104*, 405. See also: Clegg, W.; Lockhart, J. C. *J. Chem. Soc., Perkin Trans. 2* **1987**, 1621. (d) Willem, R.; Gielen, M.; Hoogzand, C.; Pepermans, H. In *Advances in Dynamic Stereochemistry*; Gielen, M., Ed.; Freund: London, 1985; p 207. (e) For a four-ring flip see: Willem, R.; Pepermans, H.; Hallenga, K.; Gielen, M.; Dams, R.; Geise, H. J. *J. Org. Chem.* **1983**, *48*, 1890. (f) Willem, R.; Hoogzand, C. *Org. Magn. Reson.* **1979**, *12*, 55. (g) Gust, D.; Mislow, K. *J. Am. Chem. Soc.* **1973**, *95*, 1535. (h) Kates, M. R.; Andose, J. D.; Finocchiaro, P.; Gust, D.; Mislow, K. *J. Am. Chem. Soc.* **1975**, *97*, 1772. (i) Glaser, R.; Blount, J. F.; Mislow, K. *J. Am. Chem. Soc.* **1980**, *102*, 2777.

(1) Stable Simple Enols. Part 19. For Part 18 see: Nadler, E. B.; Rappoport, Z.; Arad, D.; Apeloig, Y. *J. Am. Chem. Soc.* **1987**, *109*, 7873.

(2) Biali, S. E.; Rappoport, Z. *J. Am. Chem. Soc.* **1984**, *106*, 477.

(3) Kaftory, M.; Biali, S. E.; Rappoport, Z. *J. Am. Chem. Soc.* **1985**, *107*, 1701.

(4) Biali, S. E.; Rappoport, Z. *J. Org. Chem.* **1986**, *51*, 2245.

(5) For a review on helical compounds see: Meurer, K. P.; Vögtle, F. *Top. Curr. Chem.* **1985**, *127*, 1.

(6) Kurland, R. J.; Schuster, I. I.; Colter, A. K. *J. Am. Chem. Soc.* **1965**, *87*, 2279.

Table I. <sup>1</sup>H NMR Data for 1,1-Dimesitylvinyl Systems Mes<sub>2</sub>C=C(OR<sub>2</sub>)R<sub>1</sub> in CD<sub>3</sub>COCD<sub>3</sub> at 190 K and in the Coalescence Solvent<sup>a</sup>

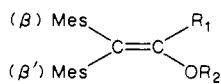
assignment/ solvent	1		2		3		4		5		6	
	CD <sub>3</sub> COCD <sub>3</sub>	CD <sub>3</sub> COCD <sub>3</sub>	CD <sub>3</sub> COCD <sub>3</sub>	CD <sub>2</sub> Cl <sub>2</sub> <sup>b</sup>	CD <sub>3</sub> COCD <sub>3</sub>	CD <sub>2</sub> Cl <sub>2</sub> <sup>c</sup>	CD <sub>3</sub> COCD <sub>3</sub>	CD <sub>2</sub> Cl <sub>2</sub> <sup>c</sup>	CD <sub>3</sub> COCD <sub>3</sub>	C <sub>6</sub> D <sub>5</sub> CD <sub>3</sub> <sup>d</sup>	CD <sub>3</sub> COCD <sub>3</sub>	CD <sub>2</sub> Cl <sub>2</sub> <sup>d</sup>
β- <i>o</i> -CH <sub>3</sub>	1.74	1.72	1.72	1.76	1.76	1.79	1.80	2.04	1.69	1.69		
β- <i>o</i> -CH <sub>3</sub>	2.46	2.43	2.45	2.43	2.48	2.41	2.56	2.61	2.56	2.55		
<i>p</i> -CH <sub>3</sub>	2.22	2.21	2.22	2.24	2.21	2.24	2.20	2.13	2.22	2.24		
β- <i>o</i> -CH <sub>3</sub>	1.70	1.75	1.78	1.78	1.81	1.79	1.84	2.09	1.72	1.73		
β- <i>o</i> -CH <sub>3</sub>	2.52	2.43	2.42	2.39	2.42	2.45	2.47	2.25	2.42	2.39		
<i>p</i> -CH <sub>3</sub>	2.21	2.20	2.20	2.25	2.20	2.24	2.20	2.09	2.22	2.25		
Mes-H	6.64	6.65	6.66	6.71	6.66	6.71	6.62	6.62	6.71	6.70		
Mes-H	6.93	6.90	6.87	6.96	6.89	6.97	6.89	6.87	6.94	6.94		
Mes-H	6.71	6.69	6.72	6.75	6.71	6.75	6.66	6.66	6.73	6.70		
Mes-H	6.97	6.97	6.91	7.00	6.99	7.00	6.91	6.87	7.00	6.99		
R <sub>1</sub>	6.63 <sup>e</sup>	1.75 <sup>f</sup>	1.10 <sup>g</sup>	1.08 <sup>h</sup>	1.08 <sup>i,k</sup>	1.06 <sup>i,k</sup>	1.07	1.33		6.27		
				2.04 <sup>l</sup>	1.15 <sup>i,k</sup>	1.11 <sup>i,k</sup>						
R <sub>2</sub>	8.84 <sup>e</sup>	7.68 <sup>l</sup>	7.44	5.04	7.44 <sup>m</sup>	4.95 <sup>n</sup>	7.37	4.98	1.23 <sup>k,o</sup>	1.27 <sup>p</sup>		
									1.27 <sup>k,o</sup>	1.29 <sup>p</sup>		4.11 <sup>q</sup>

<sup>a</sup> Unless otherwise stated, all signals are singlets. <sup>b</sup> At 195 K. <sup>c</sup> At 198 K. <sup>d</sup> At 185 K. <sup>e</sup> d, <sup>3</sup>J = 8.3 Hz. <sup>f</sup> d, <sup>4</sup>J = 1.2 Hz. <sup>g</sup> t, <sup>3</sup>J = 7.4 Hz, CH<sub>2</sub>CH<sub>3</sub>: The CH<sub>2</sub> signal overlaps one of the *p*-CH<sub>3</sub> signals. <sup>h</sup> t, <sup>3</sup>J = 7.5 Hz, CH<sub>2</sub>CH<sub>3</sub>. <sup>i</sup> q, <sup>3</sup>J = 7.5 Hz, CH<sub>2</sub>CH<sub>3</sub>. <sup>j</sup> d, <sup>3</sup>J = 6.6 Hz, CH(CH<sub>3</sub>)<sub>2</sub>. <sup>k</sup> The methine proton overlaps one of the *o*-Me signals. <sup>l</sup> q, <sup>4</sup>J = 1.2 Hz. <sup>m</sup> d, <sup>4</sup>J = 1.6 Hz. <sup>n</sup> d, <sup>4</sup>J = 1.5 Hz. <sup>o</sup> d, <sup>3</sup>J = 6.5 Hz, CH(CH<sub>3</sub>)<sub>2</sub>. <sup>p</sup> d, <sup>3</sup>J = 5.9 Hz. <sup>q</sup> m, <sup>3</sup>J = 6.5 Hz, CH(CH<sub>3</sub>)<sub>2</sub>.

to steric effects.<sup>4</sup> When Y is bulkier than hydrogen a severe steric crowding would be generated if the mesityl group *cis* to Y will pass through the double bond plane and will come in contact with Y. This steric interaction raises the energy of the transition state of the [α,β]-two-ring flip above that of the three-ring flip, making the latter the threshold mechanism.

In contrast with the triarylvinyl propellers, our knowledge of the dynamic behavior of 1,1-diarylvinyl systems is much more limited. Crystallographic data show that in the solid state these systems have a propeller conformation.<sup>9</sup> Calculations predicted that the parent compound Ph<sub>2</sub>C=CH<sub>2</sub> exists in a propeller conformation and that the rotation of the rings should be correlated.<sup>10</sup> According to these calculations, the threshold mechanism is the one-ring flip, but the transition state for the two-ring flip is only 2.6 kcal mol<sup>-1</sup> higher in energy.<sup>10</sup> Prior to the present work, no experimental data for comparison with the calculated dynamic behavior were available.<sup>11</sup>

The present work was carried out in order to find out experimentally the threshold mechanisms of 1,1-dimesitylvinyl propellers and to test whether a similar shift to that observed with trimesitylvinyl propellers would be observed if the bulk of the α substituent on the double bond is changed. We decided to focus on stable simple enols 1–5 and enol ether 6.

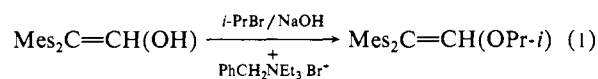


- 1: R<sub>1</sub> = R<sub>2</sub> = H      4: R<sub>1</sub> = *i*-Pr; R<sub>2</sub> = H  
 2: R<sub>1</sub> = Me; R<sub>2</sub> = H      5: R<sub>1</sub> = *t*-Bu; R<sub>2</sub> = H  
 3: R<sub>1</sub> = Et; R<sub>2</sub> = H      6: R<sub>1</sub> = H; R<sub>2</sub> = *i*-Pr

## Results

**Low-Temperature and Dynamic NMR Spectra of 1–6.** Enols 1–5 were synthesized according to the literature.<sup>12–14</sup> Enol ether

6 was synthesized by phase transfer catalyzed alkylation of 1 (eq 1). X-ray diffraction of 1–5 showed that the enols exist in the solid state in a propeller conformation.<sup>9</sup>



Compounds 1–6 displayed in the 200-MHz <sup>1</sup>H NMR spectrum in CD<sub>3</sub>COCD<sub>3</sub> at low temperature (190 K) separate signals for the OH and mostly for the methyls and aromatic protons in each mesityl ring (Table I).<sup>15</sup> Pairs of signals corresponding to ortho methyls or aromatic protons on the same mesityl ring were assigned by the saturation transfer method.<sup>2,16</sup> Assignment of the *o*-methyl signals of 1 to the β or β' ring was made as follows: as the X-ray diffraction data of 1 show, the average value of the β' torsional angle for the four crystal conformations of 1 is larger than the value of the β ring<sup>9</sup> (see Table III). Inspection of molecular models indicates that the larger twist angle of the β' ring should result in less pronounced shielding/deshielding effects of the β ring and double bond, respectively, on the *o*-methyls of the β' ring (as compared to the similar effect operating on the β ring). By this line of reasoning, the pair of *o*-methyl signals at δ 1.74 and 2.46 was assigned to the β' ring whereas the pair of signals at δ 1.70 and 2.52 was assigned to the β ring. Further support for this assignment comes from the agreement between the experimental barriers for the site-exchange process at the two rings of 1 and the calculated (molecular mechanics) rotational barriers for the different rings (see below). The number of methyl and aromatic proton signals in each compound was in agreement with a frozen (on the NMR time scale) propeller conformation in solution, although in some cases the maximum expected number of signals was not observed due to accidental isochrony of signals corresponding to a pair of diastereotopic or constitutionally heterotopic groups. For a frozen propeller conformation the two methylene protons of 3 and the two isopropyl methyls in 4 and 6 are in diastereotopic environments and should display two signals. Indeed, they appeared as separate signals for 4 (Figure 1A, Δδ = 0.07 ppm) and 6 (Δδ = 0.04 ppm) while in the case of 3 the anisochrony of the methylene proton signals could not be detected experimentally due to overlap with one of the *p*-CH<sub>3</sub> signals. The OH proton signal displayed a marked sensitivity to the R<sub>1</sub> substituent, and its chemical shift diminished along the series from δ 8.84 (for 1) to δ 7.37 (for 5).<sup>17</sup> In some of the enols a <sup>4</sup>J<sub>H-H</sub>

(9) Kaftory, M.; Nugiel, D. A.; Biali, S. E.; Rappoport, Z. Unpublished results.

(10) Stegemeyer, H.; Rapp, W. *Ber. Bunsen-Ges. Phys. Chem.* **1971**, *75*, 1165.

(11) (a) For a preliminary communication see: Nugiel, D. A.; Biali, S. E.; Rappoport, Z. *J. Am. Chem. Soc.* **1984**, *106*, 3357. (b) Presented in part at the Eighth IUPAC Conference on Physical Organic Chemistry, August 24–29, 1986, Tokyo, Japan. Rappoport, Z.; Nugiel, D. A.; Biali, S. E.; Kaftory, M. Abstract p B-27-1 and at the Swedish-Israeli Symposium: New Trends in Organic Chemistry, March 16–19, 1987, Rehovot, Israel. Rappoport, Z.; Nugiel, D. A.; Biali, S. E.; Kaftory, M. Abstract No. 41.

(12) Fuson, R. C.; Armstrong, L. J.; Chadwick, D. H.; Kneisley, J. W.; Rowland, S. P.; Shenk, W. J.; Soper, Q. F. *J. Am. Chem. Soc.* **1945**, *67*, 386.

(13) Biali, S. E.; Rappoport, Z. *J. Am. Chem. Soc.* **1984**, *106*, 5641.

(14) Nugiel, D. A.; Rappoport, Z. *J. Am. Chem. Soc.* **1985**, *107*, 3669.

(15) The <sup>13</sup>C data of enols 1–5 are displayed in Table III of ref 14.

(16) Forsên, S.; Hoffman, R. A. *J. Chem. Phys.* **1963**, *39*, 2892; **1964**, *40*, 1189; *Acta Chem. Scand.* **1963**, *17*, 1787.

**Table II.** Coalescence Data for Mes<sub>2</sub>C=C(OR<sub>2</sub>)R<sub>1</sub> at 300 MHz

	R <sub>1</sub>	R <sub>2</sub>	solvent	process	Δν, Hz	T <sub>c</sub> , K	ΔG <sup>‡</sup> , kcal mol <sup>-1</sup>
1	H	H	CD <sub>3</sub> COCD <sub>3</sub>	β'- <i>o</i> -Me ⇌ β'- <i>o</i> -Me	217	229	10.4
				β'-Mes-H ⇌ β'-Mes-H	66	215	10.3
				β- <i>o</i> -Me ⇌ β- <i>o</i> -Me	245	309	14.2
				β-Mes-H ⇌ β-Mes-H	78	293	14.2
2	Me	H	CD <sub>3</sub> COCD <sub>3</sub>	<i>o</i> -Me ⇌ <i>o</i> -Me	204	270	12.5
				<i>o</i> -Me ⇌ <i>o</i> -Me	210	270	12.5
				Mes-H ⇌ Mes-H	74	264	12.6
				Mes-H ⇌ Mes-H	84	264	12.7
3	Et	H	CD <sub>2</sub> Cl <sub>2</sub>	<i>o</i> -Me ⇌ <i>o</i> -Me	202	260	12.0
				<i>o</i> -Me ⇌ <i>o</i> -Me	185	260	12.0
				Mes-H ⇌ Mes-H	76	249	11.9
				Mes-H ⇌ Mes-H	75	249	11.9
4	<i>i</i> -Pr	H	CD <sub>2</sub> Cl <sub>2</sub>	<i>o</i> -Me ⇌ <i>o</i> -Me	185	254	11.7
				<i>o</i> -Me ⇌ <i>o</i> -Me	198	254	11.7
				Mes-H ⇌ Mes-H	77	245	11.7
				Mes-H ⇌ Mes-H	75	245	11.7
				<i>i</i> -Pr-CH <sub>3</sub> ⇌ <i>i</i> -Pr-CH <sub>3</sub> <sup>a</sup>	15	228	11.6
5	<i>t</i> -Bu	H	C <sub>6</sub> D <sub>5</sub> CD <sub>3</sub>	<i>o</i> -Me ⇌ <i>o</i> -Me	154	225	10.4
				<i>o</i> -Me ⇌ <i>o</i> -Me	185	225	10.4
				Mes-H ⇌ Mes-H	76	219	10.5
6	H	<i>i</i> -Pr	CD <sub>3</sub> COCD <sub>3</sub>	<i>i</i> -Pr-CH <sub>3</sub> ⇌ <i>i</i> -Pr-CH <sub>3</sub> <sup>a</sup>	5	208	11.0
				β- <i>o</i> -Me ⇌ β- <i>o</i> -Me	200	242	11.1
				β-Mes-H ⇌ β-Mes-H	70	232	11.1
				β'- <i>o</i> -Me ⇌ β'- <i>o</i> -Me	247	305	14.0
				β'-Mes-H ⇌ β'-Mes-H	85	294	14.1

<sup>a</sup>Coalescence of the two diastereotopic isopropyl methyl signals.

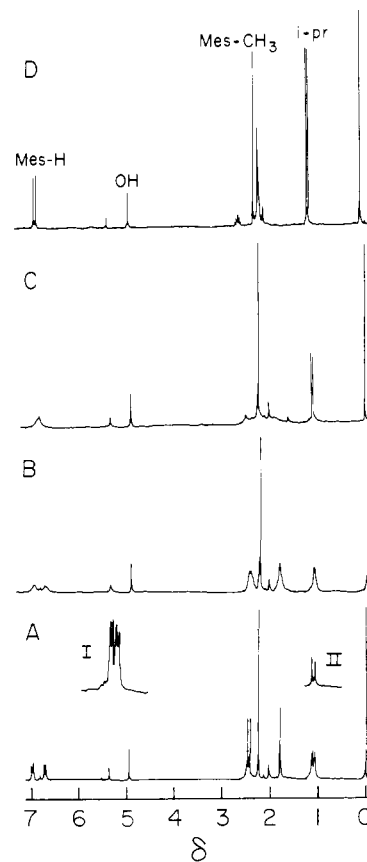
coupling constant was observed between the enolic proton and proton(s) on the R<sub>1</sub> substituent. The OH proton signal of **2** appeared as a quartet (<sup>4</sup>J<sub>H-H</sub> = 1.2 Hz) and that of **4** as a doublet (<sup>4</sup>J<sub>H-H</sub> = 1.6 Hz), while the OH signal of **3** did not show any appreciable splitting. In none of compounds **1–6** were there indications of restricted rotation about the C(sp<sup>2</sup>)-R or C(sp<sup>2</sup>)-O bonds: in all cases the <sup>1</sup>H NMR data were in agreement either with a single conformation or with a rapid interconversion of conformations, giving a single average conformation in solution. In the case of **5**, no splitting of the *t*-Bu singlet could be detected in the <sup>1</sup>H NMR down to 148 K (200 MHz, 1:1 CD<sub>2</sub>Cl<sub>2</sub>/C<sub>6</sub>D<sub>5</sub>CD<sub>3</sub>).

Upon raising the temperature several coalescence processes were observed in the NMR spectra of **1–6** (Figure 1).<sup>18</sup> In order to decrease overlap of signals, different solvents were used: CD<sub>3</sub>COCD<sub>3</sub> for **1** and **2**, CD<sub>2</sub>Cl<sub>2</sub> for **3**, **4**, and **6**, and C<sub>6</sub>D<sub>5</sub>CD<sub>3</sub> for **5** (Table I). The exchange rates at the coalescence temperatures (T<sub>c</sub>) were calculated by using the Gutowsky-Holm equation<sup>19</sup> and the rotational barriers (ΔG<sup>‡</sup>) by using the Eyring equation assuming a transmission coefficient of unity. In most cases the rotational barrier of a given ring was calculated independently from the coalescence data of the pairs of *o*-Me and aromatic protons. In general, excellent agreement was obtained between the barriers derived from the two probes. The coalescence data for **1–6** are summarized in Table II. Two types of dynamic behavior were observed. For **2–5** the measured barriers for the exchange of groups at each ring were identical. In contrast, for enol **1** and its ether **6** two different processes could be measured, each involving site exchange at a different mesityl ring. For **1**, ΔG<sup>‡</sup> values of 10.4 and 14.2 kcal mol<sup>-1</sup> were measured and for **6** the corresponding barriers were 11.1 and 14.0 kcal mol<sup>-1</sup>. In addition a barrier for the exchange of the diastereotopic isopropyl methyl groups was also measured and its value (11.0 kcal mol<sup>-1</sup>)

(17) The solvent effect on δ(OH), <sup>4</sup>J(HCCOH) and the association of the enols with the solvent are discussed in: Rappoport, Z.; Nugiel, D. A.; Biali, S. E. *J. Org. Chem.* **1988**, *53*, 4814. See also: Rappoport, Z. *Kyushu Symposium on Physical Organic Chemistry*; Fukuoka, Japan, September 1–3, 1986, Abstract on 53.

(18) The temperature dependence of the <sup>1</sup>H NMR spectrum of **5** is given in Figure 1 of ref 11a.

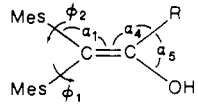
(19) Gutowsky, H. S.; Holm, C. H. *J. Chem. Phys.* **1956**, *25*, 1228.



**Figure 1.** 300-MHz <sup>1</sup>H NMR of **4** in CD<sub>2</sub>Cl<sub>2</sub>: (A) at 195 K (I, expansion of the isopropyl methyl region; II, methine-decoupled, isopropyl methyl region); (B) at 228 K; (c) at 245 K; and (D) at 293 K.

was identical (within experimental error) with the barrier for the low-energy mesityl site exchange process of **6**.

**Molecular Mechanics Calculations.** Molecular mechanics calculations were performed in order to check whether they will reproduce the geometrical parameters found for **1–5** by X-ray

**Table III.** Selected Experimental (X-ray) and Calculated (MM2(85)) Bond ( $\alpha$ ) and Torsion ( $\phi$ ) Angles of 1–5 (in Degrees)


enol	R	$\alpha_1$		$\alpha_4$		$\alpha_5$		$\phi_1$		$\phi_2^a$	
		exp	calc	exp	calc	exp	calc	exp	calc	exp	calc
1	H	118.1 <sup>b</sup>	120.3	118.1 <sup>b</sup>	120.1	113.9 <sup>b</sup>	114.8	56.7 <sup>b</sup>	57.8	50.2 <sup>b</sup>	48.4
2	Me	121.8	121.9	126.0	123.6	112.4	114.0	57.5	56.2	55.7	58.1
3	Et	119.9 <sup>c</sup>	122.5	127.3 <sup>c</sup>	123.8	109.0 <sup>c</sup>	114.2	59.7 <sup>c</sup>	55.8	58.3 <sup>c</sup>	54.7
4	<i>i</i> -Pr	120.4	122.6	127.7	123.8	110.2	114.5	62.8	55.3	60.1	57.0
5	<i>t</i> -Bu	125.4	125.4	133.2	128.1	107.4	112.6	66.0	55.8	63.7	62.6

<sup>a</sup> Torsion angles for conformations having the same helicity. <sup>b</sup> Average of values for the four symmetry independent crystallographic conformations. <sup>c</sup> Average of values for the two symmetry independent crystallographic conformations.

**Table IV.** Sites Exchanged by Flip and Nonflip Rotational Routes for 1–5

ring flip route	flipping ring	site exchanged <sup>a</sup>	rotating ring <sup>b</sup>	site exchanged <sup>a</sup>
zero-ring	[none]	(a $\bar{a}$ )(b $\bar{b}$ )(c $\bar{c}$ )(d $\bar{d}$ )(e $\bar{e}$ )(f $\bar{f}$ )	[none]	(aa)(bb)(cc)(dd)(ee)(ff)
	[ $\beta$ ]	(a $\bar{b}$ )(b $\bar{a}$ )(c $\bar{c}$ )(d $\bar{d}$ )(e $\bar{e}$ )(f $\bar{f}$ )	[ $\beta$ ]	(ab)(ba)(cc)(dd)(ee)(ff)
one-ring	[ $\beta'$ ]	(a $\bar{a}$ )(b $\bar{b}$ )(c $\bar{d}$ )(d $\bar{c}$ )(e $\bar{e}$ )(f $\bar{f}$ )	[ $\beta'$ ]	(aa)(bb)(cd)(dc)(ee)(ff)
two-ring	[ $\beta, \beta'$ ]	(a $\bar{b}$ )(b $\bar{a}$ )(c $\bar{d}$ )(d $\bar{c}$ )(e $\bar{e}$ )(f $\bar{f}$ )	[ $\beta, \beta'$ ]	(ab)(ba)(cd)(dc)(ee)(ff)

<sup>a</sup> Letters in each bracket indicate the site exchanging groups. <sup>b</sup> Rotation of a given ring by 180°.

diffraction<sup>9</sup> as well as the rotational barriers. We have shown previously that the MMP2 program predicted a reasonable geometry for (Z)-1,2-dimesityl-2-phenylethenol and reproduced satisfactorily its dipole moment.<sup>20</sup> The present calculations used the MM2(85) program<sup>21</sup> which implements Allinger's new modified torsional parameters for conjugated systems.<sup>22</sup> Selected structural parameters of the calculated structures for 1–5<sup>23</sup> are displayed in Table III, together with the corresponding experimental (X-rays) values.<sup>9</sup> In the case of 1 and 3 four and two independent conformations were found in the crystal, respectively; the values in Table III are the average for the different conformations. The calculations reproduce satisfactorily the geometrical parameters of the less crowded members of the series (1 and 2) while the deviations were largest for the most crowded enol (5). Whereas in general the calculations reproduce satisfactorily the  $\alpha_1$  and  $\phi_2$  angles, they underestimate the changes in  $\phi_1$  and  $\alpha_4$  and the narrowing of  $\alpha_5$  along the series.

Since the agreement between experimental and calculated geometries is better for 1 and 2 than for the rest of the enols, and 1 and 2 differ in their dynamic behavior, the mesityl rotational barriers were calculated for these molecules. The computations were carried out by rotating the  $\beta'$  mesityl ring from its low-energy torsional angle by the dihedral driver option of the MM2(85) program through the double bond plane or through a plane normal to it. In these processes the  $\beta$ -ring rotated concomitantly through a plane normal to the C=C plane. The calculated transition states for these processes (which resulted in enantiomerization) were 10.4 and 16.4 kcal mol<sup>-1</sup> for 1 and 27.1 and 9.1 kcal mol<sup>-1</sup> for 2.<sup>24</sup> Consequently, the calculated barriers for 1 are reasonably comparable with the experimental values (10.4 and 14.2 kcal mol<sup>-1</sup>) while for 2 the lower calculated value for one of the possible processes (9.1 kcal mol<sup>-1</sup>) is close to the experimental value (12.5 kcal mol<sup>-1</sup>).

(20) Biali, S. E.; Meyer, A. Y.; Rappoport, Z.; Yuh, Y. H. *J. Org. Chem.* **1985**, *50*, 3918.

(21) MM2(85): Allinger, N. L. *QCPE*. See also: Sprague, J. T.; Tai, J. C.; Yuh, Y. H.; Allinger, N. L. *J. Comput. Chem.* **1987**, *8*, 581.

(22) Liljefors, T.; Tai, J.; Li, S.; Allinger, N. L. *J. Comput. Chem.* **1987**, *8*, 1051.

(23) All calculations were done assuming a nonplanar  $\pi$  system (option NPLANE = 1) and a syn conformation of the OH group.<sup>24</sup>

(24) For 1 the calculations were carried out by driving the  $\beta$  ring in 10° steps and, at the high-energy region, by 2° steps. In the case of 2, driving the  $\beta$  or  $\beta'$  rings through a normal to the double bond plane resulted in a continuous increase of the steric energy. The barrier for the process was therefore estimated by mapping the steric energy as a function of the torsional angles of the two mesityl rings (using a 10° increment).

(25) One such example is chloropentakis(dichloromethyl)benzene: Biali, S. E.; Buda, A. B. *J. Org. Chem.* **1988**, *53*, 135.

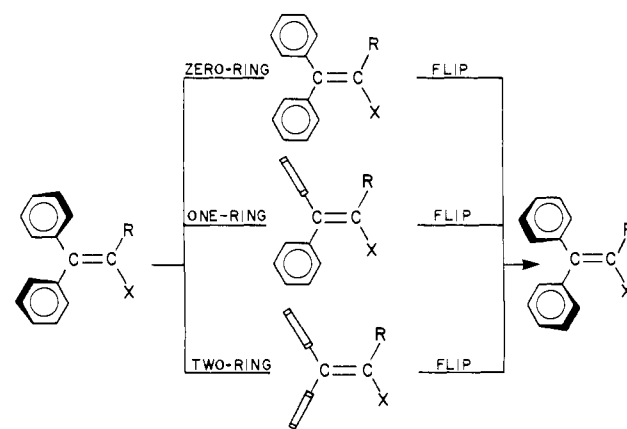


**Figure 2.** Idealized<sup>26</sup> transition states for the flip mechanism of a 2,2-diarylviny propeller. A open rectangle indicates a ring that is perpendicular to the C=C plane. The one-ring flip depicted exemplifies a [ $\beta$ ]-ring flip.

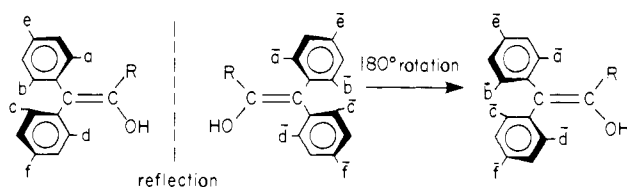


**Figure 3.** Labeling of the magnetic sites in an enantiomeric pair of 2,2-dimesitylethenols.

## Discussion

**Correlated Rotation in Vinyl Propellers.** We have previously shown that some crowded triarylethenols display identical experimental rotational barriers for the different aryl rings.<sup>2</sup> We would like to point out that our statement "the similar  $\Delta G_c^\ddagger$  values for rotation of sterically and chemically different rings is direct evidence that a correlated rotation occurs"<sup>2</sup> is strictly correct *only* if no intermediate conformers (experimentally detected or not) are present along the rotational pathway. Otherwise one could envision situations in which groups at different steric environments rotate in a noncorrelated fashion with identical measured barriers.<sup>25</sup> Consequently, ancillary information from calculations is needed in order to support a correlated mechanism or pathway.

**Rotational Mechanisms of Enols 1–5.** For a 1,1-diarylviny propeller four different mechanisms of correlated rotation (flip mechanisms) can be envisioned. The idealized transition states<sup>26</sup>

for these mechanisms are schematically depicted in Figure 2. In discussing the dynamic stereochemistry of a molecular propeller we have to consider also ring rotations ("nonflip mechanisms", consisting of rotation of a given ring by 180° without concomitant helicity reversal).

For visualizing the different site exchanges that can result from a given rotational process, the methyl groups in 1–5 are labeled a–f and their enantiotopic groups (by external comparison)<sup>27</sup> are labeled as  $\bar{a}$ – $\bar{f}$  (Figure 3). As can be seen in Figure 3, coalescence of a pair of *o*-Me groups on a given ring can be the result of a rotation of that ring by 180° (i.e., without concomitant helicity reversal) or the result of a flip of that ring. The sites exchanged resulting from the different flip and nonflip processes are summarized in Table IV (where an (ab)(ba) designation indicates a site exchange between the magnetic sites "a" and "b"). From Table IV it can be concluded that the observed site exchange for the mesityl signal of 2–5 can be explained either by a  $[\beta, \beta']$ -two-ring flip, by two successive  $[\beta]$ - and  $[\beta']$ -one ring flips, or by a rotation of both rings (either simultaneously or successively) by 180°. For 1 (or for 6 based on the coalescence of groups in the mesityl rings) the lower energy process can be explained by a  $[\beta]$ -ring flip with helicity reversal or by a 180° rotation of the  $\beta$  ring with retention of the helicity.

As Table IV shows, the zero-ring flip is the only flip route that leads to enantiomerization but does not exchange diastereotopic groups and consequently cannot be monitored by NMR. However, the possibility that this process occurs with a barrier lower than the one experimentally determined is a priori extremely unlikely since the transition state of the zero-ring flip should be extremely crowded. Unequivocal evidence supporting this conclusion was obtained by substituting 1 with a prochiral group and by comparing the rotation and enantiomerization barriers of 6.

**Exclusion of Nonflip Routes.** An experimental way that may distinguish between the flip and nonflip routes in a molecular propeller is to substitute it by a prochiral group such as isopropyl and to monitor simultaneously the site exchange due to enantiomerization (from the coalescence of the isopropyl methyls) as well as the site exchange at the aryl rings due to their rotation. If the barriers for both processes are identical, it is most likely that a single process that results in both site exchange at the rings and helicity reversal (i.e., a flip process) is being monitored. If the enantiomerization barrier is higher than the barrier for site exchange at the rings, this would indicate that the rotational process does not involve helicity reversal (a nonflip process). If, on the other hand, the enantiomerization barrier is lower in energy it would indicate that the threshold mechanism is the zero-ring flip. Using this argument nonflip routes have been previously excluded as possible threshold mechanisms of triaryl propellers.<sup>2,8c,f,28</sup>

In principle, the enantiomerization process can be monitored in 3, 4, and 6 since the diastereotopic methylene or isopropyl methyls of the R substituents can serve as enantiomerization probes, provided that the diastereotopic groups are anisochronous in the NMR spectra. Indeed, 6 was purposely prepared in order to have a system similar to 1 carrying a prochiral group. Due to peak overlap, the enantiomerization process could be detected by NMR only for 4 and 6. The identity between the enantiomerization barrier and the rotational barrier for 4 and between the enantiomerization barrier of 6 and its lower rotational barrier (Table II) indicates that the threshold mechanism belongs to the "flip" routes. Moreover, this identity experimentally excludes the possibility that enantiomerization occurs via the NMR-invisible zero-ring flip with a lower barrier than that of the monitored dynamic process.

**Threshold Mechanisms of 1–5.** As stated above, both a  $[\beta, \beta']$ -two-ring flip or two successive one-ring flips are consistent with the experimental results for 2–5. The two successive one-ring

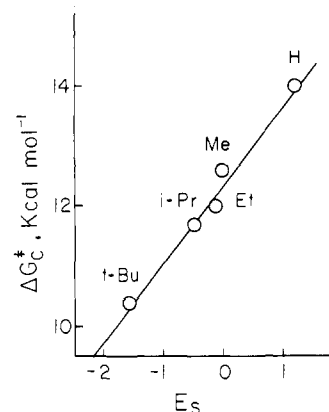


Figure 4. Plot of  $\Delta G_c^\ddagger$  for the two-ring flip process of 1–5 vs Taft's steric parameters  $E_s$ . For 1 the higher  $\Delta G_c^\ddagger$  value was used.

flips can be safely eliminated on the grounds of symmetry arguments: since the transition states for the two processes are diastereomeric they should differ in their  $\Delta G_c^\ddagger$  values. Although the possibility that two successive one-ring flips will accidentally have equal  $\Delta G_c^\ddagger$  values for one of the systems cannot be ruled out, it seems to us highly improbable that such accidental identity will occur for each one of the enols 2–5. This conclusion is strengthened by the MM2(85) calculation that predicts for 2 that the two-ring flip process should be 18 kcal mol<sup>-1</sup> lower in energy than the  $[\beta]$ -one-ring flip. Consequently, we feel safe in concluding that the threshold mechanism for 2–5 is the two-ring flip.

In the case of 1, exclusion of the non-flip routes leaves the  $[\beta']$ -one-ring flip as the only possibility for the threshold mechanism. The higher energy process (14.0 kcal mol<sup>-1</sup>) can correspond to either a  $[\beta]$ -one-ring flip or to  $[\beta, \beta']$ -two-ring flip. The similarity between the experimental value for the high-energy process and the calculated barrier for the  $[\beta, \beta']$ -two-ring flip (14.2 and 16.4 kcal mol<sup>-1</sup>, respectively) strongly suggests that the experimentally measured high barrier corresponds to a two-ring flip. This is further supported by the linear correlation found between the energy barriers for the two-ring flip process and Taft's  $E_s$  steric parameters (see below).

The shift in the threshold mechanism from a one-ring flip in 1 to a two-ring flip in 2–5 can be rationalized by steric effects. When  $R_1$  is a hydrogen, the passage of the  $\beta$  ring cis to it through the double bond plane is less hindered than other pathways, and therefore this motion is preferred over them. When  $R_1$  is an alkyl group, the corresponding steric interactions that result when the  $\beta$  ring passes through the double bond plane raise the energy of the  $[\beta]$ -one-ring flip. Concurrently, the  $\Delta G_c^\ddagger$  value of the competing two-ring flip is lowered since the alkyl substituent increases the ground-state energy by increasing the torsional angle of the rings (see below). Indeed, the barrier for the two-ring flip process decreases along the series  $\Delta G_c^\ddagger(2) > \Delta G_c^\ddagger(3) > \Delta G_c^\ddagger(4) > \Delta G_c^\ddagger(5)$ . Although the  $\Delta G_c^\ddagger$  values were determined at different solvents, we believe that the influence of the change in solvent on the barrier height is small, as previously shown for trimesityl ethenol.<sup>2</sup> Apparently, the changes at the other face of the double bond are less important, as seen by the minor difference in the  $\Delta G_c^\ddagger$  values for both processes in 1 and 6.

**Correlation of the  $\Delta G_c^\ddagger$  Values with Taft's Steric Parameters and with Structural Parameters.** The dominant role played by the  $R_1$  substituent in determining both the rotational mechanism and the magnitude of its barrier prompted us to examine whether a correlation exists between the  $\Delta G_c^\ddagger$  values and Taft's steric parameters  $E_s$ .<sup>29</sup> As shown in Figure 4 good linearity between  $\Delta G_c^\ddagger$  and  $E_s$  (correlation coefficient  $r = 0.9991$ ) is indeed obtained with a slope of -2. Especially important is that the  $\Delta G_c^\ddagger$  for the higher energy process for 1 is the value that fits the linear plot of Figure 4 thus lending further support for assigning this process

(26) In Figure 2 achiral conformations are arbitrarily chosen as transition states for the different flip mechanisms.

(27) Mislow, K.; Raban, M. *Top. Stereochem.* 1967, 1, 1.

(28) Hummel, J. P.; Gust, D.; Mislow, K. *J. Am. Chem. Soc.* 1974, 96, 3679.

(29) A compilation of  $E_s$  values using  $E_s = 0$  for hydrogen can be found in: March, J. *Advanced Organic Chemistry*, 3rd ed.; Wiley: New York, 1985; p 249.

Table V. Selected Structure/Dynamics Correlations for Enols 1-5<sup>a</sup>

equation	$r^b$	$\sigma^c$
$\Delta G_c^\ddagger = 32.12 - 0.330\phi_1$	0.92	0.08
$\Delta G_c^\ddagger = 27.77 - 0.27\phi_2$	0.99	0.01
$\Delta G_c^\ddagger = 30.50 - 0.16(\phi_1 + \phi_2)$	0.98	0.02
$\Delta G_c^\ddagger = 1.75 + 21.21 \cos \phi_1$	0.91	5.57
$\Delta G_c^\ddagger = 6.76 + 22.15 \cos^2 \phi_1$	0.92	5.37
$\Delta G_c^\ddagger = 3.63 + 16.40 \cos \phi_2$	0.99	1.02
$\Delta G_c^\ddagger = 7.85 + 15.60 \cos^2 \phi_2$	0.99	1.03
$\Delta G_c^\ddagger = 64.04 - 0.428\alpha_1$	0.84	0.16
$\Delta G_c^\ddagger = 44.24 - 0.254\alpha_4$	0.99	0.02
$\Delta G_c^\ddagger = 43.66 + 0.505\alpha_5$	0.95	0.10
$\Delta G_c^\ddagger = 12.89 - 0.048(\Delta\alpha_1)^2$	0.75	0.02
$\Delta G_c^\ddagger = 13.64 - 0.016(\Delta\alpha_4)^2$	0.95	0.003
$\Delta G_c^\ddagger = 13.34 - 0.071(\Delta\alpha_5)^2$	0.89	0.02

<sup>a</sup>  $\phi$ 's and  $\alpha$ 's are in degrees,  $\Delta G_c^\ddagger$  are in kcal mol<sup>-1</sup>. <sup>b</sup> Correlation coefficient. <sup>c</sup> Standard deviation.

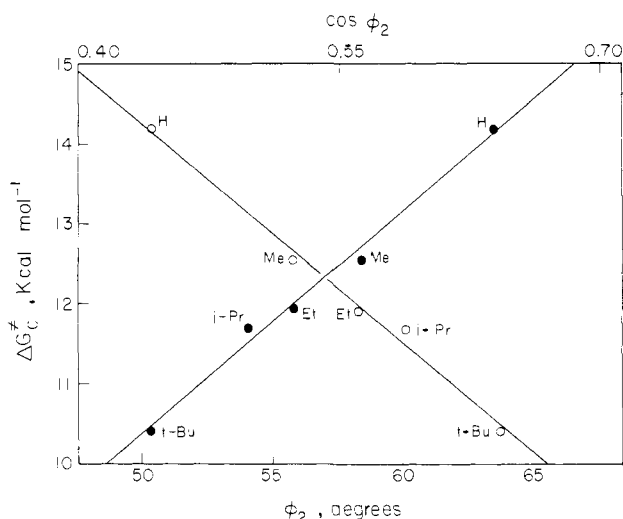


Figure 5. Plot of  $\Delta G_c^\ddagger$  for the two-ring flip process of 1-5 vs (A) the  $\phi_2$  torsional angles (bottom scale  $\circ$ ) and (B)  $\cos \phi_2$  (top scale  $\bullet$ ).

as a two-ring flip. Such a correlation can be valuable for calculating the  $\Delta G_c^\ddagger$  of the two-ring flip of a given 2,2-dimesityl-1-alkylethenol by interpolation or extrapolation, provided that the  $E_s$  parameter of the substituent is known. In summary, the linear correlation suggests that the main effect that a change in  $R_1$  has on the  $\Delta G_c^\ddagger$  values of the two-ring flip is steric.

**Structure-Dynamics Correlations.** The steric influence of the change in the substituent  $R_1$  on the rotational barriers is mainly through its influence on the ground state, as evidenced by the drop in the  $\Delta G_c^\ddagger$  values of the two-ring flip with the increase of bulk of  $R_1$ . We therefore searched for a structure-dynamics correlation<sup>30</sup> between the experimentally determined structural parameters of 1-5<sup>9</sup> and the  $\Delta G_c^\ddagger$  values. The parameters chosen for this purpose are the bond and torsional angles collected in Table III since the standard deviation of each value was smaller than its relative change along the series.<sup>31</sup> The correlations tried are summarized in Table V. It can readily be seen that poor correlations exist ( $r < 0.95$ ) between  $\Delta G_c^\ddagger$  and  $\alpha_1$  or  $\phi_1$ , a reasonable correlation exists between  $\Delta G_c^\ddagger$  and  $\alpha_5$  ( $r = 0.95$ ), and excellent correlations exist between  $\Delta G_c^\ddagger$  and  $\phi_2$  or  $\alpha_4$  ( $r = 0.99$ ). (Figures 5 and 6).

The linear correlations found for the angles themselves are somewhat surprising since one would rather expect linear correlations with  $(\Delta\alpha)^2$  (for the bond angles) or  $\cos \phi$  (for the torsional angles).<sup>32</sup> As summarized in Table V, this expectation is fulfilled

(30) For some recent examples of structure-reactivity correlations see: (a) Bürgi, H. B.; Dunitz, J. D. *Acc. Chem. Res.* **1983**, *16*, 153. (b) Allen, F. H.; Kirby, A. J. *J. Am. Chem. Soc.* **1984**, *106*, 6197. (c) Kanagasabapathy, V. M.; Sawyer, J. F.; Tidwell, T. T. *J. Org. Chem.* **1985**, *50*, 503. For a note of caution on the correlations see: Allen, A. D.; Kwong-Chip, J. M.; Mistry, J.; Sawyer, J. F.; Tidwell, T. T. *J. Org. Chem.* **1987**, *52*, 4164.

(31) This is not the case for the bond length changes along the series.

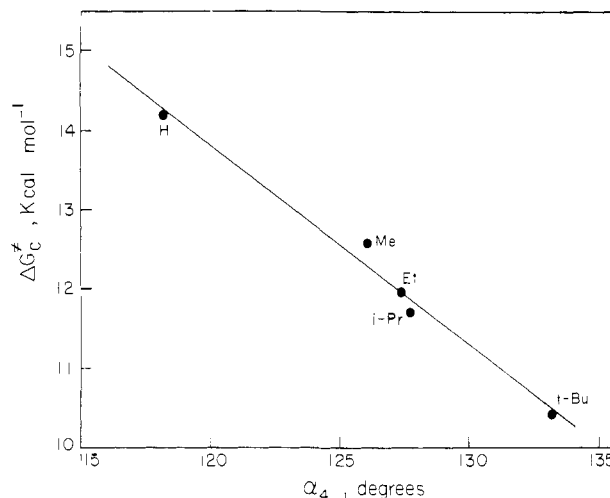


Figure 6. Plot of  $\Delta G_c^\ddagger$  for the two-ring flip process of 1-5 vs the  $\alpha_4$  bond angles.

for the torsional angle since the linearity of correlations involving  $\phi_2$  is rather insensitive to the form in which this torsional angle is expressed ( $\phi_2$ ,  $\cos \phi_2$  (Figure 5), or even  $\cos^2 \phi_2$ ). This is reflected in plots of  $\cos \phi_2$  or  $\cos^2 \phi_2$  against the  $\phi_2$  values of 1-5 which are linear with correlation coefficients larger than 0.999. Indeed, the plots of  $\Delta G_c^\ddagger$  vs  $\phi_2$  and  $\cos \phi_2$  shown in Figure 5 display quasimirror symmetry. Therefore, the linearity of the correlations with the various forms of the torsional angles results from the relatively small variation in these angles along the series. However, for  $\alpha_4$  and  $\alpha_5$  the linearity of the correlation is deteriorated when these angles are expressed as  $(\Delta\alpha)^2$  ( $\Delta\alpha$  was defined as the difference between the angle  $\alpha$  of a given enol and the corresponding angle of 1). The reason for a linear correlation with  $\alpha$  and not with  $(\Delta\alpha)^2$  is not clear although an explanation is that for calculating  $(\Delta\alpha)^2$  the  $\alpha$  angles in 1 were taken as the nondistorted (reference) angles and clearly this is only an approximation. It is likely that when more structure-dynamics (or structure-reactivity) correlations will become available, it will become clearer whether the correlation is indeed with the bond angles. A related precedent in this context is that of Allen and Kirby,<sup>30b</sup> who reported linear correlation of reaction barriers with the experimental bond lengths of the reacting molecule, although from Morse-type equations more complicated relationships should be expected.

**Calculation of Transition-State Torsional Angles.** In order to analyze the correlations found, we will assume that the transition states for the two-ring flip processes in 1-5 are of equal energy on an arbitrary scale. In this way, the difference in  $\Delta G_c^\ddagger$  values between a pair of enols in the series will represent the increase in ground-state energy along the rotational coordinate resulting by the replacement of an  $R_1$  substituent by a bulkier one. Under this assumption, the slope of the linear correlation between  $\phi_2$  and  $\Delta G_c^\ddagger$  (-0.27) represents the increase in energy (in kcal mol<sup>-1</sup>) resulting by twisting the  $\beta$  ring by 1°. It is interesting to evaluate the torsional angle  $\phi_2$  of a hypothetical enol for which the two-ring flip barrier would be essentially zero. This angle could represent a gross estimate of the torsional angle in the transition state of the two-ring flip. From the correlation between  $\Delta G_c^\ddagger$  and  $\phi_2$  (Figure 5), a torsional angle  $\phi_2 = 102 \pm 2^\circ$  can be calculated for the hypothetical transition state.

Unfortunately, the  $\Delta G_c^\ddagger$  vs  $\phi_1$  correlation was not sufficiently good to allow a similar estimate, but from the good linearity of the  $\Delta G_c^\ddagger$  vs the sum  $\phi_1 + \phi_2$  correlation ( $r = 0.98$ , Table V), the calculated value of  $\phi_1 + \phi_2$  corresponding to  $\Delta G_c^\ddagger = 0$  (our model for the transition state) is  $190^\circ$ . Notwithstanding the crudeness of our assumptions (e.g., that the  $\Delta G_c^\ddagger$  vs  $\cos \phi_2$  plot is linear over

(32) The relationship between the potential energy and angle deformations is given, in its simplest form, by the equations  $V_\phi = 1/2V_0(1 + \cos n\phi)$  (for torsional angles) and  $V_\alpha = 1/2k_\alpha(\Delta\alpha)^2$  (for bond angles). See: Mislow, K. *Introduction to Stereochemistry*; W. A. Benjamin: London, 1965; p 35.

a broad range of rotational barriers), it is interesting that by using only structural and dynamic data it can be deduced that in the transition state of the two-ring flip the two rings are nearly perpendicular to the C=C plane.<sup>33</sup>

**Relationships between Dynamic, Equilibria, and Structural Parameters.** The linear relationship between dynamic ( $\Delta G^\ddagger$ ) and structural ( $\alpha_4$ ,  $\phi_2$ , etc.) parameters is complementary to previously reported<sup>14</sup> linear correlation between the  $\Delta G^\ddagger$  and the keto  $\rightleftharpoons$  enol ( $\Delta G^\circ$ ) equilibria<sup>34</sup> for the same enols.

**Conclusions.** Replacement of the vinyl hydrogen in **1** by an alkyl group results in a shift in the threshold rotational mechanism from a one-ring to a two-ring flip. The present work and the similar complementary behavior observed for trimesitylvinyl systems<sup>4</sup> suggest that when the double bond substituent is small the passage of the ring cis to it through the C=C plane becomes energetically feasible. Consequently there is a shift in threshold mechanism from (*n*)-aryl ring flip to (*n* - 1)-aryl ring flip. This is in contrast with Ar<sub>3</sub>CX molecular propellers where the threshold mechanism was consistently the two-ring flip.<sup>8</sup>

(33) Note that if the transition-state conformation of the two-ring flip is chiral, it should exist in two enantiomeric forms. A similar calculation to that described above but using the enantiomeric conformations of **1-5** should result in an enantiomeric (if the transition state is chiral) or identical (if the transition state is achiral) conformation.

(34) The caption of the linear  $\Delta G^\circ$  vs  $\Delta G^\ddagger$  plot displayed in Figure 2 of ref 14 is erroneously exchanged with that of Figure 3.

## Experimental Section

Infrared spectra were taken with a Perkin-Elmer 157 G spectrometer. <sup>1</sup>H NMR spectra were recorded on a Bruker WP 200 SY and WH-300 pulsed FT spectrometer equipped with an Aspect 2000 computer. Temperature measurements were based on the chemical shift separation of the protons of a methanol sample and utilization of the temperature shift correlation of Van Geet.<sup>35</sup>

**2,2-Dimesitylvinyl Isopropyl Ether (6).** To a solution of 2,2-dimesitylethanol (120 mg, 0.4 mmol) and benzyltriethylammonium bromide (25 mg, 0.1 mmol) in 2-bromopropane (5 mL), a solution of 50% aqueous NaOH (5 mL) was added, and the mixture was stirred at room temperature overnight. Ether (20 mL) was then added, the phases separated, and the organic phase washed with water (2 × 10 mL), dried (MgSO<sub>4</sub>), and evaporated. The residue was recrystallized from ethanol to give colorless crystals (80 mg, 67%) of **6**: mp 125-6 °C;  $\nu_{\max}$  (Nujol) 1650 cm<sup>-1</sup>; MS, *m/z* 322 (M, 72%), 280 (B, Me<sub>2</sub>C=CHOH<sup>+</sup>). Anal. Calcd for C<sub>23</sub>H<sub>30</sub>O: C, 85.66; H, 9.38. Found: C, 85.88; H, 9.54.

**Acknowledgment.** We are indebted to Dr. L. Radom for helpful discussions. This work was supported by a grant from the United States-Israel Binational Science Foundation (BSF) Jerusalem, to whom we are grateful.

**Registry No.** **1**, 54288-04-9; **2**, 89959-15-9; **3**, 96040-90-3; **4**, 96040-91-4; **5**, 89959-16-0; **6**, 118071-22-0.

(35) Van Geet, A. L. *Anal. Chem.* **1968**, *40*, 2227; **1970**, *42*, 679.

## Comparison of Classical Simulations of the H + H<sub>2</sub> Reaction to Accurate Quantum Mechanical State-to-State Partial Cross Sections with Total Angular Momenta *J* = 0-4 and to Experiment for All *J*

Meishan Zhao,<sup>†</sup> Mirjana Mladenovic,<sup>†</sup> Donald G. Truhlar,<sup>\*,†</sup> David W. Schwenke,<sup>‡</sup> Yan Sun,<sup>⊥</sup> Donald J. Kouri,<sup>⊥</sup> and Normand C. Blais<sup>||</sup>

*Contribution from the Department of Chemistry, Chemical Physics Program, and Supercomputer Institute, University of Minnesota, Minneapolis, Minnesota 55455, Eloret Institute, Sunnyvale, California 94087, Department of Chemistry and Department of Physics, University of Houston, Houston, Texas 77204-5641, and Chemistry Division, Los Alamos National Laboratory, Los Alamos, New Mexico 87545. Received May 31, 1988*

**Abstract:** Quantum mechanical calculations are reported for probabilities and partial cross sections for the reaction H + *p*-H<sub>2</sub> (*v* = 0, *j* = 0, 2, *E*<sub>rel</sub> = 1.1 eV, *J* = 0-4) → *o*-H<sub>2</sub> (*v*' = 0, 1) + H, where *v*, *j*, and *v*' are initial vibrational, initial rotational, and final vibrational quantum numbers, respectively, *E*<sub>rel</sub> is the initial relative translational energy, and *J* is the conserved total angular momentum quantum number. The calculations involve three arrangements and 468-780 coupled channels, and they are converged to 0.1-1%. The corresponding quantities are also calculated by the quasiclassical trajectory method, and comparing these results provides a detailed test of the trajectory method. For most final states, the trajectory results agree with the quantal ones within a factor of 1.5 to 2, and the trajectory value for the (*v*' = 1)/(*v*' = 0) branching ratio is too high by a factor of 1.6. We also report trajectory results that are converged with respect to increasing *J*, and the converged value of the branching ratio is found to be 2.5 times larger than experiment.

### 1. Introduction

Classical dynamical simulations are of great usefulness and interest in all branches of chemical dynamics.<sup>1-5</sup> The calculated results are often reasonable; in very few cases, however, has it been possible to test the absolute accuracy of classical methods for molecular collisions. The exception concerns atom-diatom and

diatom-diatom collisions in the gas phase, for which the classical simulations take the form of the quasiclassical trajectory (QCT) method with semiclassical state initialization and histogram binning or smooth sampling algorithms for final-state assignment.<sup>6</sup>

(1) Marcus, R. A. In *Energy Storage and Redistribution in Molecules*; Hinze, J., Ed.; Plenum: New York, 1983; p 573.

(2) Raff, L. M.; Thompson, D. L. In *Theory of Chemical Reaction Dynamics*; Baer, M., Ed.; CRC Press: Boca Raton, FL, 1985; Vol. 3, p 1.

(3) Truhlar, D. G.; Dagdigan, P. J. *Comments At. Mol. Phys.* **1986**, *17*, 335.

(4) McCammon, J. A. *Repts. Progr. Phys.* **1984**, *47*, 1.

(5) Hynes, J. T. *Annu. Rev. Phys. Chem.* **1985**, *36*, 573.

<sup>†</sup> University of Minnesota.

<sup>‡</sup> Eloret Institute. Mailing address: NASA Ames Research Center, Mail Stop 230-3, Moffett Field, CA 94036.

<sup>⊥</sup> University of Houston.

<sup>||</sup> Los Alamos National Laboratory.